Thermal Analysis and Heat Exchanger Design for Pulse Detonation Engine

by

Hari Narayanan Nagarajan and Frank K. Lu

reprinted from

International Journal of
Aerospace Innovations

Volume 1 · Number 3 · September 2009

Multi-Science Publishing
ISSN 1757-2258

Thermal Analysis and Heat Exchanger Design for Pulse Detonation Engine

Hari Narayanan Nagarajan[a] and Frank K. Lu[b]
Mechanical and Aerospace Engineering Department, University of Texas at Arlington, Arlington, Texas 76019-0018, USA
Corresponding author: franklu@uta.edu

ABSTRACT

The thermal environment of a pulse detonation engine was modeled using a space-time averaging procedure. The method allowed the one-dimensional, lumped-capacitance model to be used. The tube dimensions were a bore of 100 mm and a length of 1 m. For the calculations, the PDE pulse was split into a heating, exhaust and purging subprocess. Assumptions for the duration of each process were made based on previous experiments. The PDE was also assumed to operate at about 19 Hz. The calculations were performed for a stoichiometric air and octane mixture initially at STP. Wall materials consist of stainless steel, copper and Haynes alloy. Different water flow rates and jacket radii were used. The study showed that high water flow rates and large jackets were able to reduce the temperature at the water jacket. The temperatures of the inner and outer PDE walls were unaffected by the coolant flow or the jacket dimensions. These surfaces remain at high temperatures and indicate that a PDE requires advanced cooling techniques. For this configuration with stainless steel surfaces, the PDE wall temperatures were still rising albeit slowly after 12000 cycles.

NOMENCLATURE

a	acoustic speed
A	circumferential area
$Bi = h\Delta r/k$	Biot number based on duct thickness
CEA	Chemical Equilibrium with Applications (code)
CJ	Chapman–Jouguet
c_p	specific heat capacity at constant pressure
D_{CJ}	speed of Chapman–Jouguet detonation wave
D_H	hydraulic diameter
$Fo = \alpha t/L_c^2$	Fourier number based on the characteristic length, defined as the ratio of the volume to circumferential area
h	heat transfer coefficient
k	thermal conductivity
k_A	thermal conductivity of PDE chamber tube and the water jacket
L	length of the detonation chamber
L_c	characteristic length
M_{CJ}	Chapman–Jouguet detonation Mach number
Nu	Nusselt number
p	pressure
PDE	pulse detonation engine
$Pr = \mu c_p/k$	Prandtl number
q	heat developed per unit mass
$\dot{Q}$	rate of heat transfer by coolant

[a]Graduate Research Assistant. Email: hari.nagarajan@mavs.uta.edu.

[b]Professor, Email: franklu@uta.edu.

r	radius
$r^* = r/r_a$	dimensionless radial coordinate
R	thermal resistance
Re	Reynolds number
t	time
T	temperature
U	overall heat transfer coefficient
V	velocity of the gas flow
x	axial distance from the closed end
α	thermal expansion coefficient
γ	specific heat ratio
θ^*	dimensionless temperature distribution
μ	fluid viscosity
ρ	density
Subscripts	
a,b,c,d	inner and outer surface of PDE chamber, and inner and outer surface of water jacket
amb	ambient
ca	coefficient for air
cd	coefficient for detonation
cw	coefficient of water
cyc	cycle
d, *det*	detonation
e	exit of heat exchanger
ex	open-end boundary of rarefaction wave originating from open end
exh	exhaust
fill	fill
g	gas
i	inlet of heat exchanger
purge	purge + fill
w	wall
wa	inner surface of PDE chamber
wb	outer surface of PDE chamber
wc	inner surface of water jacket
wd	outer surface of water jacket
1	undisturbed state of the detonable mixture
2	Chapman–Jouguet condition of detonation wave; also, detonation wave location
∞	ambient surroundings

1. INTRODUCTION

Pulse detonation engines (PDEs) have received much interest lately because of their theoretically higher thermodynamic efficiency over conventional gas turbine engines and their simplicity in construction and operation, amongst other advantages.[1] The PDE utilizes the energy release from repeated detonations and is thus a cyclic device where each cycle can be divided simply into four processes, namely, filling, detonation, exhaust and purging. These processes are shown in Fig. 1. This figure shows that the propellants are first injected from the closed end on the left-hand side of the tube at a relatively low speed. The mixture is then ignited. In this paper, it is assumed that a detonation wave is formed instantaneously that propagates at the Chapman–Jouguet velocity. The high pressure from the detonation wave produces thrust. A nozzle, if attached at the end of the tube, will increase the thrust due to the expanding flow. For simplicity in this analysis, a nozzle is not included since the interest here is restricted to the heat transfer that arises from the detonation. After the detonation wave exits the tube, an exhaust phase that consists of an unsteady rarefaction propagates into the tube from the open end to scavenge it. This phase occurs if the unsteady Taylor expansion following the

detonation wave is below the ambient pressure and, thus, may not necessarily occur. The inrush of ambient air helps to cool the detonation tube. However, this is generally insufficient to lower the tube temperature to below the autoignition level of the reactants. A purge of the tube is therefore required by pumping in cool air. The tube is now ready for a fresh charge of reactants and the cycle repeats itself. While these processes shown in Fig. 1 are somewhat simplistic, they capture the major processes that are pertinent for this analysis without introducing further complications. The processes described above form a "unit cycle" which can be conveniently displayed in a displacement-time diagram, as shown in Fig. 2. The figure depicts qualitatively the duration of each of the four processes. The propagating detonation wave takes up the shortest amount of time but is obviously critical for thrust production and, as it turns out, it creates a large amount of heat.

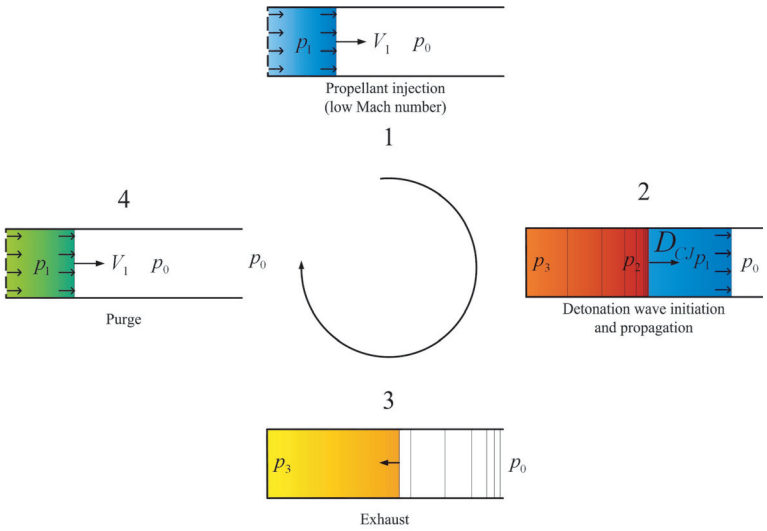

Figure 1. A representative PDE cycle

While much of the research has focused on producing reliable detonations at high frequencies, the practical implementation of PDEs requires the solution of numerous engineering issues, including thermal management. The rapid energy release from a detonation in a small volume implies that the heating rates are very high. Experiments have shown that the heating can be very severe even for a short duration of a few seconds.[2] Hoke et al.[3] measured heating rates for a 50 mm bore by 0.91 m long detonation tube constructed of Schedule 40 aluminum. The tube was jacketed by another Schedule 40 aluminum tube with a bore of 63.5 mm. Water flowed in the annulus between the two tubes to provide cooling. The heat load due to the pulsed detonation was obtained from a thermal balance between in inlet and outlet of the water flow. Hoke et al.[3] found heating rates of about 21 kW for detonations in stoichiometric, hydrogen-air mixtures of 20 Hz. For an uncooled tube, these authors found that the detonation tube reached thermal equilibrium in about two minutes. A temperature variation of 170 K existed along the length of the tube. The hottest part of the tube is toward the end of the deflagration-to-detonation transition and reached about 815 °C. These observations were qualitatively confirmed by Panicker et al.[2] who measured exhaust temperatures of about 800 °C and who found that the water-cooled tube reached equilibrium in a shorter time. Without cooling, Panicker et al.[2] found structural damage to the PDE, including thermal expansion, destruction of the Shchelkin spiral used to speed up deflagration-to-detonation transition, and burning of seals. Bazhenova and Golub[4] stated that heat flux densities of 0.6 MW/m^2 at pulse frequencies of 40–50 Hz can rise to 2–2.5 MW/m^2 at frequencies of 200 Hz. Besides experimental observations, analytical studies have been carried out to study the effect of sensible heat release and heat loss on pulse detonation engine performance parameters.[5,6] The possibility of thermal fatigue from repeated heat pulses has also been investigated.[7]

Despite the importance of the high heating upon the PDE structure, not much attention has been paid to cooling techniques. While most PDEs are presently operating as ground demonstrators, any flightweight design must consider cooling methods carefully. Implementing effective heat removal methods for the high heating rates mentioned above can be a challenge. The heat transfer problem is

complicated by the cyclic nature of the flow processes in a pulse detonation chamber. This paper presents a preliminary analysis of the heating and cooling requirements of a PDE. While detailed analysis will eventually be necessary for design improvements, the present analysis is deemed to be adequate for preliminary sizing of a heat exchanger.

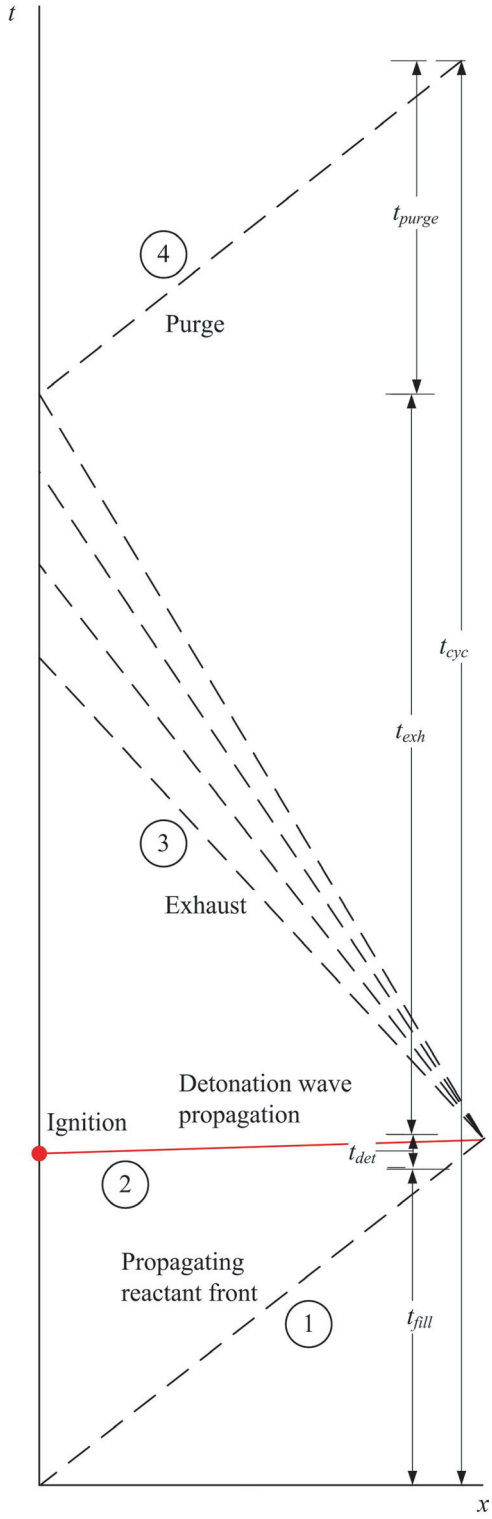

Figure 2. The ideal unit process for a pulse detonation engine with end wall fill and purge.

2. METHODOLOGY

A water-jacket heat exchanger is proposed to ensure the structural integrity of the detonation tube under severe heating. Such heat exchangers are well developed and easy to implement although complications in the design procedure can arise from the high-frequency, high heat pulses from the cyclic detonation process. A preliminary heat transfer analysis is carried out analytically as a precursor to the design of heat exchanger. The method is based on an approach developed by Endo and Fujiwara[8,9] in their analysis of PDE performance. It can be noted that a simplified analysis was given by Byrd et al.,[10] where there is no heat exchanger and where the heating and cooling pulses were assumed to be purely sinusoidal.

To simplify the thermal analysis, the heat exchanger is considered to be a concentric circular duct with constant cross section surrounding the detonation tube, as shown schematically in Fig. 3. The detonation chamber is closed at one end and opened at the other, as described earlier with reference to Fig. 1. The flow in the heat exchanger jacket is assumed to be one dimensional and constant. For the present analysis, whether the heat exchanger is co- or counter-flow is not considered.

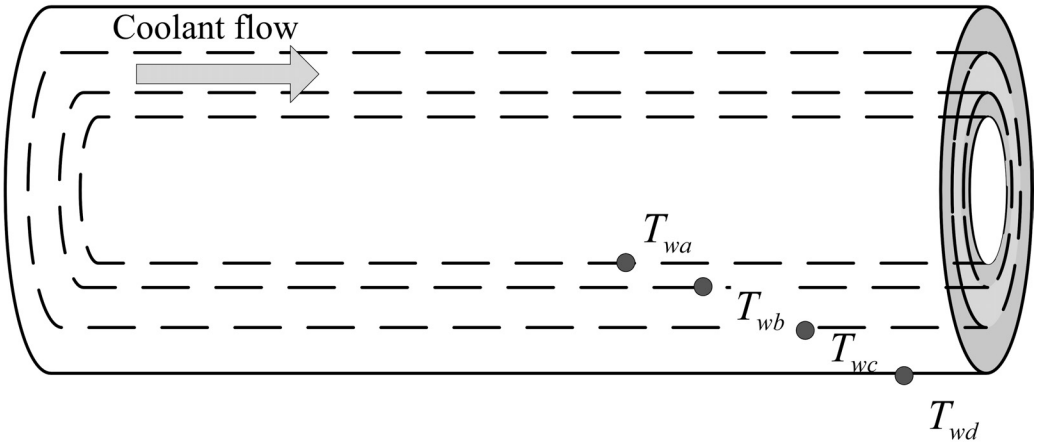

Figure 3. Schematic of cooling arrangement for pulse detonation engine.

The thermal analysis makes use of the lumped capacitance method.[11,12] The design choices such as water flow rate and the sizing of the heat exchanger were determined from the analysis.

The single PDE pulse can split into four distinct and independent processes, namely, (i) filling, (ii) detonation and (iii) exhaust and (iv) purging. However, for the present analysis, the temperature of the purge and fill gases is the same so these two subprocesses can be combined. Thus,

$$t_{cyc} = t_{det} + t_{exh} + t_{purge} \tag{1}$$

where the subscript *purge* implies both purging and filling; in other words, for heating considerations, only three subprocesses are needed. (Deflagration-to-detonation transition (DDT) is neglected in this analysis. When DDT is present, its primary contribution in the thermal-structure analysis is to lengthen the tube. It has also been found experimentally that the DDT section is hotter than the rest of the tube[2] and will require a further separate study in the future.) The present approach simplifies the analysis by removing the inherent unsteadiness in the problem in assuming a series of steady subprocesses. Strictly, the subprocesses are propagating transients and approximated by space-time averaging. For example, the tube may be filled from the closed end in certain PDE arrangements and the reactant front then propagates to the open end. This procedure, which will be described later, provides average values within each subprocess.

2.1. Time-averaged properties of the subprocesses

2.1.1. Post-Detonation Properties

The reactants used for the analysis are octane and air in a stoichiometric mixture initially at 298.15 K and 101.325 kPa. In practice, it is expected that the initial temperature will be higher to vaporize the liquid fuel. The post-detonation properties were obtained with the CEA code.[13,14] The post-detonation pressure, temperature and specific ratio are 1864 kPa, 2834 K and 1.16 respectively. The CJ speed and Mach number are 1786 m/s and 5.40 respectively. Since the ignition and DDT processes are ignored, the duration of the detonation subprocess is 0.56 ms.

The state of the flow at any location behind the detonation front is given by the following relations[8,9]

$$\rho(x) = \left(\frac{1}{\gamma_2} + \frac{\gamma_2 - 1}{\gamma_2} \frac{x}{x_2} \right)^{2/(\gamma_2 - 1)} \rho_2 \tag{2}$$

$$p(x) = \left(\frac{1}{\gamma_2} + \frac{\gamma_2 - 1}{\gamma_2} \frac{x}{x_2} \right)^{2\gamma_2/(\gamma_2 - 1)} p_2 \tag{3}$$

$$a = a_2 - \frac{\gamma_2 - 1}{\gamma_2 + 1} \frac{x_2 - x}{t} \tag{4}$$

The temperature can be obtained from (2) and (3) and the perfect gas law. The coordinate is measured from the closed end to the open end and x_2 is the distance of the detonation wave from the closed end. Data obtained from the CEA code are used along with the above three equations and the ideal gas relation to obtain the pressure, density, temperature data for various time and space input.

The histories of the pressure, density and temperature are shown in Fig. 4.[8,9] The Taylor expansion has been discretized into one to four segments to simplify the analysis, depending on the location of the detonation wave. The figure shows that the properties at any location in the tube, such as the temperature, vary with time. For example, the left end of the tube where the detonation wave is initiated will sustain a longer temperature soak than the right end. Consider the gas temperature at a location x in the tube $T_{det}(x,t)$, $0 \le x \le L$. The average temperature at x due to the detonation wave can be expressed as

$$\bar{T}_{det}(x) = \frac{1}{t_{det}} \int_0^{t_{det}} T(x,t)\, dt \tag{5}$$

The average temperature of the entire tube during the detonation phase is then

$$\tilde{T}_{det} = \frac{1}{L} \int_0^L \bar{T}_{det}(x)\, dx \tag{6}$$

Equations (5) and (6) thus represent the space-time averaging that simplifies the analysis. An important observation of Fig. 4 is that the temperature level does not decay much during the Taylor rarefaction compared to the rapid decay of pressure or density.

2.1.2. Unsteady Rarefaction Properties

A similar space-time averaging method as for the propagating detonation wave is used for the unsteady rarefaction process. The duration of the rarefaction process is arbitrarily set to 3 ms based on experiments.[2] The state of the gas during rarefaction is obtained by the following relations[9]

$$\rho(x) = \left(1 + \frac{\gamma_2 - 1}{D_{CJ}} \frac{L - x}{t - t_1}\right)^{2/(\gamma_2 - 1)} \rho_{ex} \tag{7}$$

$$p(x) = \left(1 + \frac{\gamma_2 - 1}{D_{CJ}} \frac{L - x}{t - t_1}\right)^{2\gamma_2/(\gamma_2 - 1)} p_{ex} \tag{8}$$

$$\rho_{ex} = \frac{\gamma_2 + 1}{\gamma_2^{2\gamma_2/(\gamma_2 - 1)}} \rho_1 \tag{9}$$

$$p_{ex} = \frac{\gamma_2 + 1}{\gamma_2^{2\gamma_2/(\gamma_2 - 1)}(\gamma_2 + 1)} M_{CJ}^2 p_1 \tag{10}$$

The blowdown temperature is obtained by assuming a temporally quadratic decay of pressure and temporally cubic decay of density. The temperature, pressure and density decays in the detonation tube due to the passage of the rarefaction wave are plotted in Fig. 5. The profiles are taken at 1, 1.8 and 3.6 ms after the exit of the detonation wave. The figure shows that these values reached an almost uniform level 3.6 ms after the detonation wave exits the tube. It can be noted that the temperature still remains high in the tube. Further, it can also be noted that this process is quite slow compared to the detonation wave propagation.

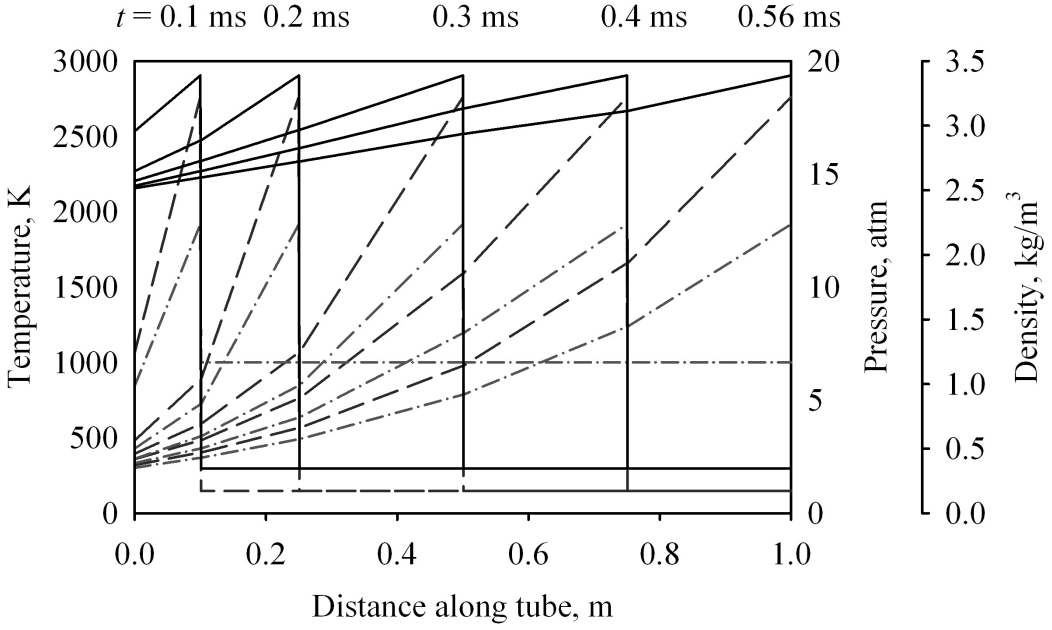

Figure 4. Unsteady properties of propagating detonation wave. The profiles are at t = 0.1, 0.2, 0.3, 0.4 and 0.56 ms; solid line: pressure, dashed line: density, dot-dashed line: temperature.

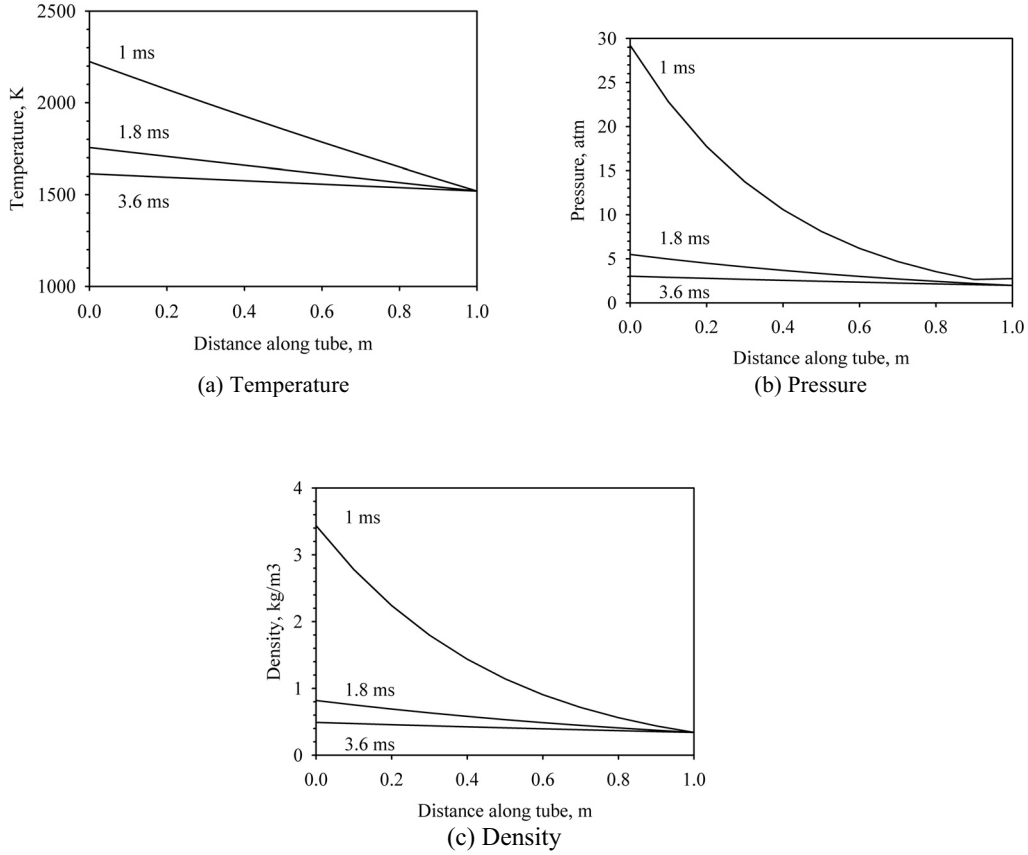

Figure 5. Properties of rarefaction wave at various times after the exit of the detonation.

2.1.3. Purging

Owing to the heat transfer due to the exhaust gas and also from the walls, the average value of purge temperature is assumed to be 400 K and the purge time is taken to be 50 ms. This is the slowest process of all.

2.2. Heating analysis

The heat developed during the detonation process is computed using

$$q = \left(c_p T + \frac{V^2}{2} \right)_e - \left(c_p T + \frac{V^2}{2} \right)_i \tag{11}$$

where the subscripts *i* and *e* refer to the inlet and exit of the detonation tube. Following from the averaging procedure above, the Reynolds number of the gas flow based on the tube diameter is found to be $Re = 2.45 \times 10^5$. The space-time average values of the kinematic viscosity and the velocity are 1×10^{-4} m^2/s and 242 m/s respectively. This value of the Reynolds number implies that the flow in the detonation tube, on average, is turbulent. Thus, the Dittus-Bolter correlation[10] is employed to obtain the heat transfer coefficient of the gas flow in the PDE duct during the detonation phase:

$$h = \frac{k}{D_H} Nu \tag{12}$$

where the Nusselt number is given as

$$Nu = 0.023 Re^{0.8} Pr^{0.4} \tag{13}$$

2.2.1. Lumped capacitance method

The lumped capacitance method is used for estimating the wall temperatures T_{wa}, T_{wb}, T_{wc} and T_{wd} for the three subprocesses of detonation, rarefaction and purging. The innermost wall temperature T_{wa} is obtained from[11]

$$\frac{T - T_\infty}{T_i - T_\infty} = \theta^* = f\left(r^*, Bi, Fo\right) \tag{14}$$

Here,

$$\theta^* = \theta_0^* \cos(\zeta_1) \tag{15}$$

where

$$\theta_0^* = \sum_{n=1}^{\infty} C_n \exp(-\zeta_n^2 Fo) J_0(\zeta_n r^*) \tag{16}$$

$$C_n = \frac{2}{\zeta_n} \frac{J_1(\zeta_n)}{J_0^2(\zeta_n) + J_1^2(\zeta_n)} \tag{17}$$

and where $J_0(\zeta_n)$ and $J_1(\zeta_n)$ are Bessel functions of the first kind and their values are obtained by assuming a plane wall for this case. Further the values of ζ_n are obtained by solving[11]

$$\zeta_n \frac{J_1\left(\zeta_n\right)}{J_0\left(\zeta_n\right)} = Bi \tag{18}$$

The assumption of a plane wall is reasonable considering that the wall thickness-to-radius ratio is small. The one-term approximation of equations (16–17) is used with equation (14) to obtain the wall temperatures T_{wa} and T_{wb} for each process, namely, detonation, rarefaction and purging.

The calculations were performed for a detonation tube with an internal diameter of 0.1 m and a length of 1 m. Variations in tube materials, water flow rates and wall thicknesses were considered. The materials considered were AISI 304 stainless steel, copper and Haynes alloy. For simplicity, material properties at 800 K were used. For AISI 304 steel, the values of density and thermal conductivity are 7900 kg/m^3 and 22.6 W/m.K, for copper the respective values are 8933 kg/m^3 and 366 W/m.K, and for Haynes alloy the respective values are 8290 kg/m^3 and 26.1 W/m.K. The water flow rate was varied from 0.125–2 kg/s which resulted in a turbulent flow in all cases.[15] The computed values of the Biot number was less than 0.1 so that the error in using the lumped capacitance method is small. Finally, the cycle-averaged temperature $\tilde{T}_{wa}$ and $\tilde{T}_{wb}$ are obtained.

2.2.2. Thermal analogy method

Once the space-time averaged heat flux to the wall is known, the thermal analogy method is used to determine the wall temperatures. The thermal circuit for analyzing the one-dimensional heat flux is shown in Fig. 6. The equations to be solved here are

$$\dot{Q} = UA\Delta T$$

$$\frac{1}{UA} = \frac{1}{2\pi r_a L h_{det}} + \frac{\ln\left(r_b/r_a\right)}{2\pi k_A L} + \frac{1}{2\pi r_c L h_{water}} + \frac{\ln\left(r_d/r_c\right)}{2\pi k_A L} + \frac{1}{2\pi r_d L h_{\infty}} \tag{19}$$

where $\Delta T = T_{wd} - T_{wa}$ is the overall temperature difference. In Eqn. (19), h_{∞} is the convective heat transfer coefficient of the ambient air around the water jacket and it is assumed to be 10 W/m^2.K.

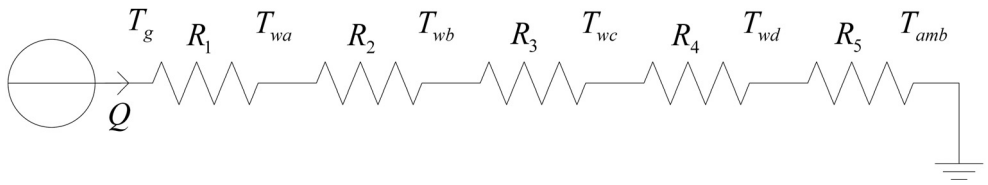

Figure 6. Thermal circuit.

2.2.3. Multi-cycle calculation method

The procedure above for the single-cycle calculation is repeated for studying multiple cycles as encountered in a pulse detonation engine. The gas temperature is modeled using the space-time average temperature data of each subprocess obtained for the single cycle. For single cycle,

$$T_{wa} = f\left(T_{gas}\right) = f\left[\frac{1}{3}\left(\int_0^{t_{\det}} T_{\det} + \int_{t_{\det}}^{t_{exh}} T_{exh} + \int_{t_{rarefy}}^{t_{purge+fill}} T_{purge/fill}\right)\right] \tag{20}$$

Hence, for n cycles,

$$T_{wa}^{n} = \sum_{cycle=1}^{n} f\left(T_{gas}\right) = \sum_{cycle=1}^{n} f\left[\frac{1}{3}\left(\int_0^{t_{\det}} T_{\det} + \int_{t_{\det}}^{t_{exh}} T_{exh} + \int_{t_{rarefy}}^{t_{purge+fill}} T_{purge/fill}\right)\right] \tag{21}$$

The temperature T_{wb} can be obtained analogously.

3. RESULTS AND DISCUSSION

3.1 Single-cycle analysis

In the calculations, the fully-developed detonation wave propagates through the tube in 0.56 ms. Based on a plausible profile, the rarefaction is assumed to last for 3 ms while the purge was assumed to last for 50 ms.[2] The cycle time is therefore about 53.6 ms, corresponding to a cycle frequency of 18.7 Hz. This is somewhat low and a higher frequency can be obtained by reducing the purge time.

The temperatures obtained from the space-time averaging approach are shown in Table 1. The table shows that the Biot numbers of steel and Haynes alloy for the present conditions are comparable while that of copper is much lower. The table also shows that the inner and outer wall temperatures are approximately the same for the three choices of wall material.

The heat release is found to be 0.186 MW. The wall temperatures for different water flow rates, wall thicknesses of the heat exchanger tube and materials are displayed in Table 2. The table shows that the range water flow rates do not affect the wall temperatures. This is expected because of the relatively short residence time of the detonation pulse. Increasing the radius of the detonation tube reduces the temperature due to the larger area for heat transfer.

Table 1. Time and space averaged temperature of the inner and outer walls of the detonation tube.

(a) Steel

	Detonation	Rarefaction	Purge
Duration (ms)	0.56	3	50
Bi	0.089		
T_{gas} (K)	1777	1661	400
T_{wa} (K)	1458	1367	378
T_{wb} (K)	1445	1355	377
Average T_{wa} (K)	1067		
Average T_{wb} (K)	1059		

(b) Copper

	Detonation	Rarefaction	Purge
Duration (ms)	0.56	3	50
Bi	0.032		
T_{gas} (K)	1777	1661	400
T_{wa} (K)	1570	1470	386
T_{wb} (K)	1567	1467	386
Average T_{wa} (K)	1142		
Average T_{wb} (K)	1140		

(c) Haynes alloy (H282)

	Detonation	Rarefaction	Purge
Duration (ms)	0.56	3	50
Bi	0.089		
T_{gas} (K)	1777	1661	400
T_{wa} (K)	1433	1345	376
T_{wb} (K)	1417	1330	375
Average T_{wa} (K)	1051		
Average T_{wb} (K)	1041		

Table 2. Wall temperatures with variation in surface area, and water flow rate for stainless steel pipe.

Water flow rate kg/s	ID of water jacket (in)	OD of water jacket (in)	T_{wa} (K)	T_{wb} (K)	T_{wc} (K)	T_{wd} (K)
0.4	0.13	0.14	1067	1059	1049	1048
0.7	0.13	0.14	1067	1059	1053	1052
1.0	0.13	0.14	1067	1059	1054	1053
0.45	0.15	0.17	1067	1059	1030	1029
0.7	0.15	0.17	1067	1059	1038	1037
1.0	0.15	0.17	1067	1059	1043	1042
0.5	0.20	0.22	1067	1059	972	971
0.7	0.20	0.22	1067	1059	991	989
1.0	0.20	0.22	1067	1059	1006	1005

(b) Copper

Water flow rate kg/s	ID of water jacket (in)	OD of water jacket (in)	T_{wa} (K)	T_{wb} (K)	T_{wc} (K)	T_{wd} (K)
0.4	0.13	0.14	1142	1140	1129	1129
0.7	0.13	0.14	1142	1140	1133	1133
1.0	0.13	0.14	1142	1140	1135	1134
0.45	0.15	0.17	1142	1140	1108	1108
0.7	0.15	0.17	1142	1140	1117	1117
1.0	0.15	0.17	1142	1140	1123	1123
0.5	0.20	0.22	1142	1140	1043	1043
0.7	0.20	0.22	1142	1140	1064	1064
1.0	0.20	0.22	1142	1140	1082	1082

(c) Haynes alloy

Water flow rate kg/s	ID of water jacket (in)	OD of water jacket (in)	T_{wa} (K)	T_{wb} (K)	T_{wc} (K)	T_{wd} (K)
0.4	0.13	0.14	1051	1041	1031	1030
0.7	0.13	0.14	1051	1041	1035	1033
1.0	0.13	0.14	1051	1041	1036	1035
0.45	0.15	0.17	1051	1041	1013	1011
0.7	0.15	0.17	1051	1041	1021	1019
1.0	0.15	0.17	1051	1041	1026	1024
0.5	0.20	0.22	1051	1041	956	954
0.7	0.20	0.22	1051	1041	974	972
1.0	0.20	0.22	1051	1041	990	988

3.2. Multi-cycle analysis

An example of multi-cycle analysis performed with stainless steel is discussed. The PDE frequency is 19Hz and the waterflow rate used for multiple cycle analysis is 0.4 kg/s. The study was carried up to 200 thousand cycles. The calculation revealed that there is a rapid temperatures increase initially. The rate of temperature increase slows down with time. The gradual increase in temperature after a large number of cycles corroborates the trend observed in experiments.[10] The temperatures obtained from this multiple cycle computation as a function of cycles of PDE operation are given in Fig. 7. The results show that the temperature increases gradually with number of cycles of operation albeit at a slower rate beyond 12000 cycles. Oscillatory nature of the flow-field does have the effect on determination of the cooling flow requirement and the multi-cycle analysis is carried to show it explicitly.

The accuracy of any simplified model can only be vouched via comparison with experiment. No comparisons were possible at the moment but, instead, the procedure elaborated here was used to help design a PDE. It was felt that the general trends are in line with the previous, referenced studies. Comparison with data is definitely desired and we propose to refine this model based on future tests.

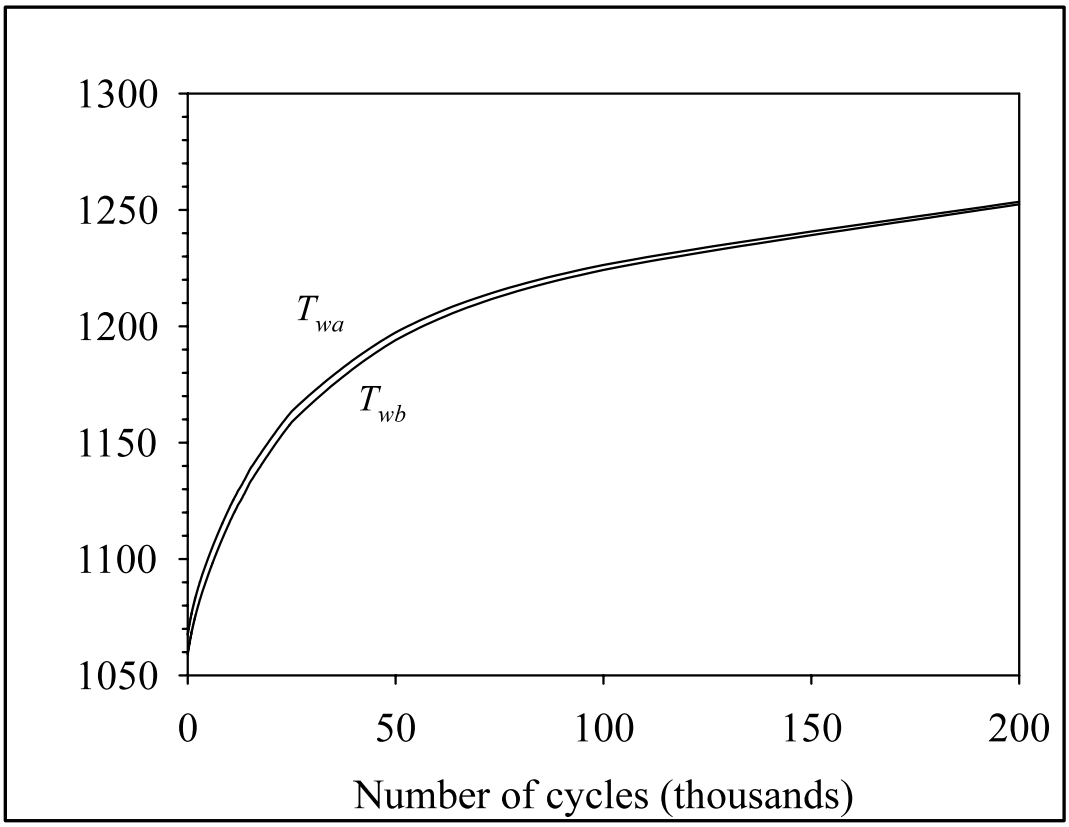

Figure 7. Temperature of inner and outer walls of PDE with number of cycles.

4. CONCLUSIONS

The heat transfer in a pulse detonation engine, 1 m long and 100 mm bore, operating at 19 Hz was analyzed for stoichiometric octane/air. The detonation tube was cooled by a water jacket with turbulent flow. A space-time averaging procedure was used in the analysis. This approach provides an indication of the final equilibrium state of the thermal condition of the walls. Various materials, tube radii and water flow rates were considered. The different materials did not have a significant effect on the surface temperatures. An increase in surface area brought about by a larger diameter heat exchanger, increased the heat transfer and reduced the wall temperature. Another result from this analysis is that the high heat release even at such a low operating frequency causes extremely hot walls. The temperature kept rising although at a slower rate even after 12000 cycles. The study shows that increasing the operating frequency will require a better cooling strategy.

ACKNOWLEDGEMENTS

The authors gratefully acknowledge funding through a Research Collaboration Agreement with the National University of Singapore. They also thank Prof. D.R. Wilson and Dr. P.K. Panicker for numerous useful discussions.

REFERENCES

1. Kailasanath, K., Review of propulsion applications of detonation waves, *AIAA Journal*, Vol. 38, No. 9, 2000, pp. 1698–1708.
2. Panicker, P.K., Lu, F.K. and Wilson, D.R., Practical issues in ground testing of pulsed detonation engines, IMECE 2007–44068, 2007.
3. Hoke, J., Bradley, R., and Schauer, F., Heat transfer and thermal management in a pulsed detonation engine, AIAA Paper 2003–6486, 2003.
4. Bazhenova, T.V. and Golub, V.V., Use of gas detonation in a controlled frequency mode (review), *Combustion, Explosion and Shock Waves*, Vol. 39, No. 4, 2003, pp. 365–381

5. Povinelli, L.A., Impact of the dissociation and sensible heat release on pulse detonation and gas turbine engine performance, ISABE 2001-1212; also, NASA/TM–2001–211080.
6. Radulescu, M.I., and Hanson, R.K., Effect of heat loss on pulse-detonation-engine flow fields and performance, *Journal of Propulsion and Power*, Vol. 21, No. 2, 2005, pp. 274–285.
7. Zhu, D., Fox, D.S., Miller, R.A., Ghosn, L.J. and Kalluri, S., Effect of surface impulsive thermal loads on fatigue behavior of constant volume propulsion engine combustor materials, *Surface and Coatings Technology*, Vols. 188–189, 2204, pp. 13–19.
8. Endo, T. and Fujiwara, T., A simplified analysis on a pulse detonation engine model, *Transactions of the Japan Society for Aeronautical and Space Sciences*, Vol. 44, No. 146, 2002, pp. 217–222.
9. Endo, T. and Fujiwara, T., Analytical estimation of performance parameters of an ideal pulse detonation engine, *Transactions of the Japan Society for Aeronautical and Space Sciences*, 2003, Vol. 45, No. 150, pp. 249–254.
10. Byrd, W.L., Schauer, F, Hoke, J.L. and Bradley, R., Lumped-Capacitance Model of a Tube Heated by a Periodic Source with Application to a PDE Tube, in M. Kutz, ed., *Heat-Transfer Calculations*, McGraw-Hill, Chapter 10.
11. Mills, F.A., *Basic Heat and Mass Transfer*, Richard D Irwin, Inc., Chicago, 1995.
12. Incropera, F.P. and DeWitt, D.P., *Fundamentals of Heat and Mass Transfer*, 5th ed., Wiley, New York, 2002.
13. McBride, B.J. and Gordon, S., Computer program for calculation of complex chemical equilibrium compositions and applications I. Analysis, NASA-RP1311, October 1994.
14. McBride, B.J. and Gordon, S., Computer program for calculation of complex chemical equilibrium compositions and applications II. User's manual and program description, NASA-RP1311-P2, June 1996.
15. Dou, H.-S., Khoo, B.C. and Tsai, H.M., Critical condition for flow transition in a full-developed annulus flow, arXiv:physics/0504193, 2005